Applied Catalysis B: Environmental 174–175 (2015) 120–125

Contents lists available at ScienceDirect

Applied Catalysis B: Environmental

journal homepage: www.elsevier.com/locate/apcatb

Insight into CO_2 methanation mechanism over NiUSY zeolites: An *operando* IR study

A. Westermann[a], B. Azambre[b], M.C. Bacariza[a], I. Graça[a], M.F. Ribeiro[a], J.M. Lopes[a], C. Henriques[a,*]

[a] CQE, Centro de Química Estrutural, Instituto Superior Técnico, UTL, Av. Rovisco Pais, 1049-001 Lisboa, Portugal
[b] Université de Lorraine, Laboratoire de Chimie et Physique Approche Multi-échelle des Milieux Complexes (LCPA2MC), EA 4632, Institut Jean Barriol, Rue Victor Demange, 57500 Saint-Avold, France

ARTICLE INFO

Article history:
Received 9 December 2014
Received in revised form 16 February 2015
Accepted 20 February 2015
Available online 21 February 2015

Keywords:
Infrared *operando* spectroscopy
Ni-based zeolite
Mechanism
Formates
Carbonyls

ABSTRACT

Ni-impregnated USY zeolites with increasing Ni content (5, 10, 14%$_{wt.}$) were investigated by *operando* IR spectroscopy for both CO_2 adsorption and CO_2 methanation conditions reaction. *In-situ* FTIR and TPD experiments highlighted a rather weak CO_2 adsorption, which occurs namely as carbonates or CO_2 linear complexes over cations (*e.g.*, Na^+). Under methanation conditions, dissociated hydrogen reacts with carbonates and/or physisorbed CO_2, leading to monodentate formates, then carbonyls (both adsorbed onto Ni^0 particles), and finally to methane. A detailed *mechanism* of the pathways involved in CO_2 methanation over NiUSY catalysts is then discussed in accordance with infrared spectroscopic data.

© 2015 Elsevier B.V. All rights reserved.

1. Introduction

Nowadays, CO_2 emissions arising from fossil fuels are becoming more and more critical for the ecosystem regarding the greenhouse gases effect. Important amounts of CO_2 are emitted from electric power plants consuming coal or natural gas, industrial plants (such as cement works) but also from engine-powered vehicles [1]. In order to limit the man's fingerprint on the climate change, the European Commission tries to regulate these emissions by reducing the CO_2 production by 60–80% toward 2050 [2]. Nevertheless, world CO_2 emissions could exceed 37 Gt/year by 2035 [3]. Among several solutions including CO_2 capture and storage (CCS), CO_2 hydrogenation appears to be one of the possible sustainable solutions to reach EU objectives, since it represents an interesting source of carbon to produce oxygenates and/or hydrocarbons [1,4–6]. The produced hydrocarbons (namely methane) can be either used as synthetic substitute of natural gas (SNG) [7] or as a source of energy in power plants, creating a global cycle between CH_4 combustion and CO_2 hydrogenation.

In this way, CO_2 hydrogenation has been studied over a wide range of supports [8–12] (*e.g.*, SiO_2, Al_2O_3, TiO_2, Ce–Zr mixed oxides) and using VIIIB metals (*e.g.*, Rh [13], Ru [9,14], Pd [15] and Ni [11,12]). Among this wide variety of supports and metals studied, few attention has been paid for Ni/zeolite catalysts despite an interesting catalytic activity with [16] or without plasma-assistance [12]. In fact, our former results [12] showed that NiUSY zeolites could promote CO_2 hydrogenation into methane with conversions and selectivities comparable to those found for the best CO_2 methanation catalysts reported in the literature [11], that use potentially more expensive bulk cerium oxide supports.

Despite several studies focused on the mechanism [10,11,17], the active surface species and reaction pathways are still under debate according to the used support and metallic specie but also the reaction conditions (T°, concentration of reactants, presence of active sites, etc). On the one hand, adsorbed CO formed by direct dissociation or disproportionation onto nickel metallic particles [18] or by partial reduction of carbonate and/or formate intermediates [19], is considered as the "true" intermediate involved in the CH_4 formation. The CO formation by direct dissociation is thought to occur exclusively on metallic species such as Rh or Ni [16], whereas the formation of carbonates implies such adsorption/activation sites of CO_2 (*i.e.*, basic sites) [10]. The adsorbed CO can be further dissociated into adsorbed C and O, which are hydrogenated respectively to CH_4 and H_2O [17]. The pathway involving direct dissociation of CO_2, corroborated by DFT studies [16], does not totally match with the CO_2 methanation. Indeed, the presence of H_2 in

* Corresponding author. Tel.: +351 218419288.
E-mail address: carlos.henriques@ist.utl.pt (C. Henriques).

http://dx.doi.org/10.1016/j.apcatb.2015.02.026
0926-3373/© 2015 Elsevier B.V. All rights reserved.

the gas feed is important only after the CO dissociation, whereas other DFT [20] and experimental [10] studies have highlighted the formation of products such as formates, which are energetically more favorable than the direct dissociation. In addition, mechanisms involving CO as intermediate do not take into account the competitive Reverse Water Gas Shift (RWGS) reaction, which leads to the formation of CO_2 and H_2. On the contrary, this mechanism can explain in part why in studies using FTIR spectroscopy, no other clear evidence than the CO formation can be observed on IR spectra.

On the other hand, Solymosi et al. [19] assume that the CO hydrogenation is negligible on Rh/Al_2O_3 and rather indicate that adsorbed oxygenate type species ($C_xH_yO_z$) such as formates are thought to be hydrogenated until CH_4 formation [11]. In this mechanism, metallic species such as Rh or Ni have the primary role to produce active hydrogen atoms by dissociating H_2. It implies that formation of CO (adsorbed onto active sites) will be detrimental for the hydrogenation by blocking metallic sites. Reducing directly oxygenate type species implies also the presence of basic sites (considered here as active sites) which do not have to be too strong in order to be reactive at temperature below 500 °C. In this way, Pan et al. [10] have studied the promotion effect of medium basic sites for the CO_2 methanation over Ni/ceria–zirconia and $Ni–Al_2O_3$ catalysts. They propose that medium basic sites enhance the activity by promoting the formation of monodentate formate, which is thought to be more active. Nevertheless, this mechanism presents three main drawbacks: i) the metallic particle has to be close to the active site for the H spillover; ii) the active site has to be able to adsorb/activate CO_2 to form oxygenate type species ($C_xH_yO_z$); iii) this mechanism does not explain how the C—O cleavage occurs.

Regarding our former results presenting conversion and selectivities close to the best catalysts found in the literature, some information relative to intermediates and actives sites are now mandatory to understand which are the key parameters. Hence, this work is devoted to understand which mechanism previously cited occurs for the CO_2 hydrogenation under stoichiometric conditions (CO_2/H_2 = 1:4) over Ni-impregnated zeolites by using *operando* FTIR spectroscopy. This study is based on an IR cell, which allows us to follow simultaneously both the gas and the adsorbed phase while increasing the reactor temperature. In addition, to fully understand the reaction route, we will try to elucidate which intermediate between CO and oxygenate type species is really active. Regarding the CO formation, the CO_2 adsorption/desorption was studied both in absence and in presence of H_2 to highlight its origin. Finally, the use of a USY zeolite (with a low Si/Al ratio and an acidic behavior) is thought to limit the adsorption of carbon dioxide. Since this catalyst presents a rather high activity, we will try to find which site is the active site involved in this reaction.

2. Experimental

2.1. Catalyst preparation

The ultra-stable Y (USY) zeolite was supplied by Grace Davison (unit cell formula $Na_{17}H_{21}Al_{38}Si_{154}O_{384}$, 16.5 EFAL), which is around 45% Na exchanged (2.1%$_{wt.}$). The Ni introduction on the zeolite support was carried out by incipient wetness impregnation (5–14 wt.%), using nickel nitrate hexahydrate ($Ni(NO_3)_2{\cdot}6H_2O$, Merck, >99%) as precursor salt diluted in a water volume close to that of the zeolite pores and added drop by drop to the zeolite. The suspension was kept under stirring while adding the precursor solution. After Ni impregnation, catalysts were dried overnight at 80 °C then calcined at 500 °C for 6 h under dry air flow (60 mL × min^{-1} × g^{-1}). The prepared catalysts are referred as *x*% NiUSY (*x* = Ni content).

2.2. Catalyst characterization

CO_2-TPD was carried out in a fixed-bed flow reactor. The catalyst (*m* = 200 mg) was reduced *in-situ* at 470 °C for 1 h under H_2 flow (80% balanced with N_2), then flushed under N_2 and cooled down to 50 °C under the same atmosphere. Then, the gas mixture was switched to pure CO_2 for 30 min until the adsorption equilibrium was reached. After that, the excess adsorptive gas was purged with an N_2 flow for 30 min, the catalyst was heated up to 700 °C at a rate of 10 °C × min^{-1} in the N_2 flow, and desorbed species were analyzed using a CO_x Siemens Ultramat 23 infrared detector.

2.3. Operando *IR measurements*

Operando IR spectra were collected using an IR cell from In-Situ Research Instruments, coupled to a Nicolet 6700 spectrometer equipped with MCT detector, by recording 50 scans at a resolution of 4 cm^{-1}. The different catalysts were pressed into a 16 mm diameter self-supported wafers of around 20 mg and were first reduced *in-situ* at 450 °C for 1 h under a flow of 20 mL × min^{-1} composed by 20% H_2/Ar. Samples were then cooled down by steps to 150 °C while recording different background spectra. Then, the reduced samples were exposed to the appropriate reactive mixture (CO_2/Ar (5/95) or CO_2/H_2/Ar (5/20/75)) for 30 min at 150 °C and the temperature was then increased up to 450 °C while maintaining a total flow rate of 20 mL × min^{-1}. All gases were supplied by Air Liquide, with purities ≥99.9990%. Difference spectra corresponding to the adsorbed species were obtained by subtracting those corresponding to the reduced fresh sample to those obtained under reactive conditions at the same temperatures.

3. Results and discussion

3.1. Catalytic activity for the methanation reaction

The behavior of the NiUSY zeolites for CO_2 methanation was already evaluated in our previous study [12]. Hence, only the most important aspects are reported here. From Fig. 1-B, the maximum activity for CO_2 methanation was obtained at 450 °C for all catalysts. The CO_2 conversions jump from 44.9 to 72.6% (Fig. 1-B) with methane selectivities between 60 and 95% (not shown here) when increasing the Ni content from 5 to 14%$_{wt.}$ By contrast, the parent USY zeolite was not active for CO_2 hydrogenation. These increases in conversion and selectivity were attributed to the higher amount of nickel oxide (NiO) particles located on the outer surface, which are reduced as Ni^0 after pre-treatment under H_2 at 470 °C. Only a minor part remains as Ni^{2+} in exchangeable positions and/or NiO in the internal cavities of the zeolite.

3.2. CO_2-TPD

CO_2 thermodesorption experiments under inert atmosphere were achieved in order to obtain complementary information on the relative amounts and adsorption strengths of ad-species generated upon the exposure of the different NiUSY zeolites to carbon dioxide. CO_2 being a weak Lewis acid, its adsorption usually increases with the surface basicity [21]. CO_2-TPD profiles in Fig. 1-A show that, depending on desorption temperature and the amount of impregnated Ni, catalysts exhibit different adsorption sites, classified arbitrarily thereafter as weak, medium and strong. Due to their very weak stabilities, physisorbed CO_2 is not expected to contribute to the signals observed between 100 and 550 °C (Fig. 1-A). CO_2-TPD profiles of the USY and 5% NiUSY zeolites were found to be rather flat, indicating the poor behavior of those samples to adsorb carbon dioxide. By contrast, the 10% NiUSY and 14% NiUSY catalysts display broad CO_2 desorption profiles, in the range of weak

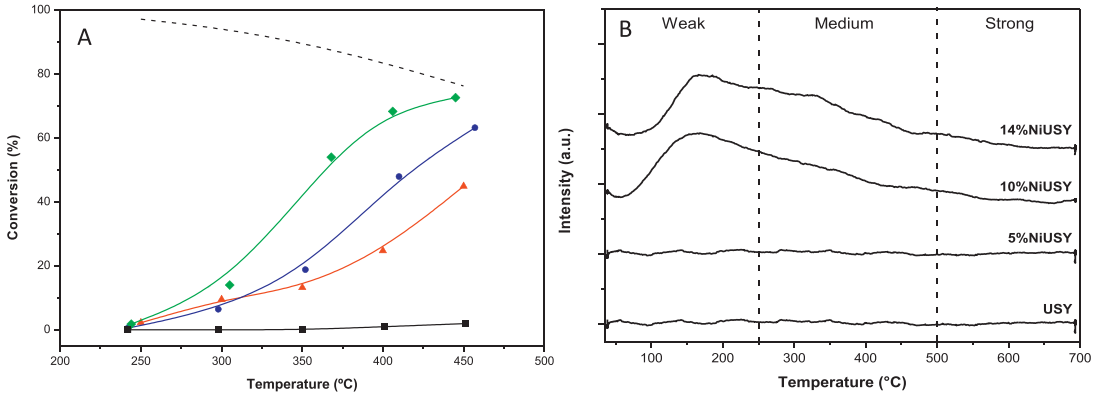

Fig. 1. - (A) Steady-state CO_2 conversion *vs.* temperature under gas mixture composed by H_2:CO_2:N_2 (molar ratio 36:9:10) at GHSV = 43,000 h^{-1} and a total flow rate of 250 mL/min for the USY (■), 5% NiUSY (▲), 10% NiUSY (●) and 14% NiUSY (♦) catalysts. Dashed line – thermodynamic equilibrium conversion values [12]; (B) CO_2-TPD profiles for (a) USY, (b) 5% NiUSY, (c) 10% NiUSY and (d) 14% NiUSY zeolites. (For interpretation of the references to color in this figure legend, the reader is referred to the web version of this article.)

and medium adsorption sites. In line with other studies [21], these signals arise from the desorption of various forms of carbonates (or CO_2 linear complexes) having weak to moderate thermal stability and adsorbed namely on (O-terminated) Ni metallic sites or unreduced NiO particles. As we will see, these sites are expected to be involved in CO_2 methanation due to a concordance between desorption temperatures and catalyst activation. More details on CO_2 ad-species is given in the forthcoming section.

3.3. FTIR measurements

In order to explain the increasing CO_2 methanation with the Ni content and the methanation mechanism, IR *operando* measurements have been carried out under CO_2 and CO_2/H_2 mixtures from 150 to 450 °C.

CO_2 adsorption. On Fig. 2-A, are presented the FTIR spectra corresponding to CO_2 adsorption after 30 min at 150 °C on USY and NiUSY (with Ni content ranging from 5 to 14%$_{wt.}$). First, it has to be acknowledged that the most important contribution to the 1635 cm^{-1} band arises from a (H—O—H) bending mode of adsorbed water (present as impurity or by-product in our system) onto the USY support [22]. The shoulder at 1610 cm^{-1} appears only in presence of nickel (Fig. 2-A, spectra a–d) and seems to be sensitive to the Ni loading and is observed both on reduced (spectra b–d) and unreduced catalysts (spectrum a). Without certainty, the band at 1610 cm^{-1} can be assigned to some perturbation of the bridged OH groups after Ni addition. The formation of an absorption band at around 1383 cm^{-1} is due to the symmetric stretch of adsorbed OCO—M^{x+} linear complexes [23]. It is worth noting, that in the gas-phase, this vibration is IR inactive but becomes IR active when CO_2 is adsorbed in the zeolite due to interaction with cations (*e.g.*, Na^+) [23]. In addition, the weak band observed around 1276 cm-1 is attributed to a combination band arising from Fermi resonance between the Raman-active ν_1 symmetric vibration and the overtone of the bending mode ν_2 ($2\nu_2$) [23]. The negative absorption observed around the cut-off limit (near 1200–1150 cm^{-1}, not shown here) is due to a perturbation of surface metal–oxygen bonds and has also been consistent with the existence of CO_2 adsorbed molecularly [24]. Nevertheless, other contributions to the broad absorptions *ca.* 1375 cm^{-1} can be also attributed to the ν_3(O—C—O)$_s$ of carbonates linked with ν_3(O—C—O)$_{as}$ modes around 1430 cm^{-1} (or in the range 1700–1600 cm^{-1}) over NiUSY and 1470 cm^{-1} over USY zeolite (ν_3(O—C—O)$_{as}$). These bands could be attributed to the formation of monodentate carbonates adsorbed on extra framework aluminum (EFAL) or Ni^0 particles present on the external surface [23–27]. Overall, it can be seen an increase of the adsorbed amount of CO_2 with the nickel content, as revealed earlier by CO_2-TPD (Fig. 1-A).

Operando IR spectra under temperature-programmed surface reaction (TPSR) conditions over the 14% NiUSY zeolite following the CO_2 uptake are presented in Fig. 2-B. All bands associated to adsorbed water and carbonate-like/CO_2 linear complexes strongly decrease above 200 °C, revealing rather weak interactions with the surface, in agreement with other studies [24,27]. From only in presence of Ni) start to appear with maxima at 1537, 1448 and 1360 cm^{-1} (Fig. 2-B, 250–450 °C). Bands at 1537 and 1360 cm^{-1}

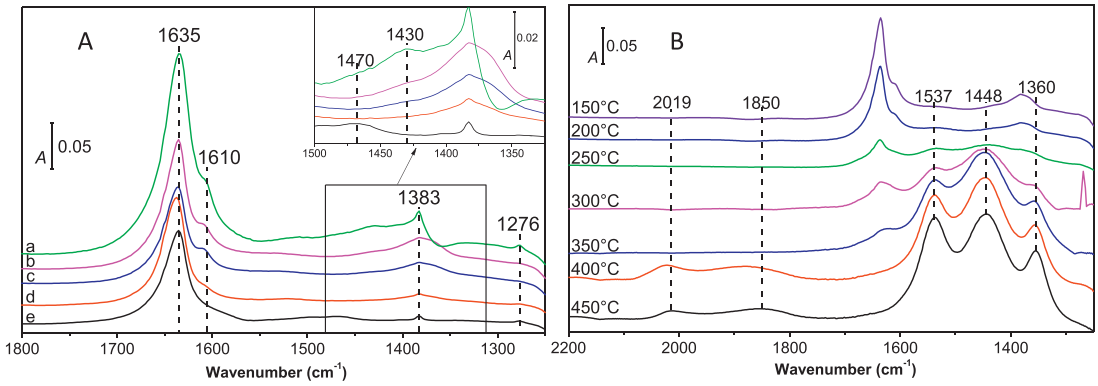

Fig. 2. - FTIR spectra recorded at 150 °C for (A) CO_2 adsorption after 30 min: (a) fresh 14% NiUSY, (b) 14% NiUSY, (c) 10% NiUSY, (d) 5% NiUSY and (e) USY zeolites; (B) TPSR under CO_2/Ar after saturation of the 14% NiUSY sample. (For interpretation of the references to color in this figure legend, the reader is referred to the web version of this article.)

have been attributed by Gallei et al. [28] to bidentate carbonates on Ni^{2+} from the remaining NiO in the supercages whereas the band centered at 1448 cm^{-1} is assigned to "free" bulk carbonates from a carbonated nickel phase. As expected, these species have high thermal stabilities and are not removed upon evacuation at 450 °C, in absence/presence of hydrogen (Fig. 3). Anticipating the forthcoming results obtained in methanation condition, these bulk carbonates appear to be only "spectator" species with no participation in the methanation mechanism. Finally bands related to adsorbed carbonyls onto Ni^0 sites are visible from 400 °C (bands at 2019 and 1850 cm^{-1} on Fig. 2-B)). Hence, the above-mentioned results can be possibly depicted by the CO_2 disproportionation (Eq. (1)) or CO_2 dissociation (Eq. (2)) on the metallic surface with re-oxidation of reduced nickel (Eq. (3)) [29]:

$$2CO_2 \rightarrow CO_{(ads)} + CO_{3(ads)} \quad (1)$$

$$CO_2 \rightarrow CO_{(ads)} + O_{(ads)} \quad (2)$$

$$Ni^0 + O_{(ads)} \rightarrow NiO \quad (3)$$

Methanation conditions. *Operando* IR spectra obtained in the course of CO_2 methanation over USY and NiUSY zeolites are presented in Fig. 3. Typical adsorbed species are still observed at 150 °C (Fig. 3, spectrum a) on USY and 5% NiUSY such as adsorbed water and carbonates/CO_2 linear complexes. On the contrary, from nickel contents above $10\%_{wt.}$ novel absorption bands become apparent at 1573 cm^{-1} as well as a doublet at 1391 and 1351 cm^{-1}. These bands can be attributed to monodentate formates adsorbed onto Ni^0 particles [30]. Considering the results presented above, surface formates can arise from a surface reaction between dissociated hydrogen and physisorbed or adsorbed perturbed CO_2 molecules [20], such as in:

$$CO^-_{2(ads)} + H_{(ads)} \rightarrow HCOO^-_{(ads)}. \quad (4)$$

Concomitantly to the progressive formates depletion with the temperature, surface carbonyls on metallic sites are also produced, as witnessed by the absorptions observed at 2061 (di-carbonyls), 2034 (mono-carbonyls), 1902 and 1823 cm^{-1} (bridged carbonyls) [11]. It is worth noting that carbonyls are formed at much lower temperatures under CO_2/H_2 (Fig. 3) than in absence of hydrogen (Fig. 2). Hence, their production cannot be simply explained by CO_2 disproportionation/dissociation reaction. Rather, it is known from the literature that adsorbed formates onto Ni surface are not stable and react according to [20,31,32]:

$$HCOO_{(ads)} \rightleftharpoons HCO_{(ads)} + O_{(ads)} \rightleftharpoons CO_{(ads)} + OH_{(ads)} \quad (5)$$

Concerning the carbonyls, it is interesting to note a modification of their relative populations according to the temperature (Fig. 3, 14% NiUSY). In that way, mono-carbonyls increase at the expense of bridged and di-carbonyls. This observation seems to be logical, considering that bridged and di-carbonyls are less stable than mono-carbonyls while increasing the carbonyl population or the temperature.

Finally, we were able to observe directly in the IR cell the methane production over 14% NiUSY in gas phase from 250 °C (as witnessed by its typical absorptions at 1310 and 3010 cm^{-1} (not shown here)). This is very consistent with catalytic data shown in Fig. 1-B.

With an effort to better describe the evolution of adsorbed and gaseous species in function of the temperature, the Fig. 4 represents the relative evolution of adsorbed formates and carbonyls as well as the relative concentration of gaseous CH_4 detected by

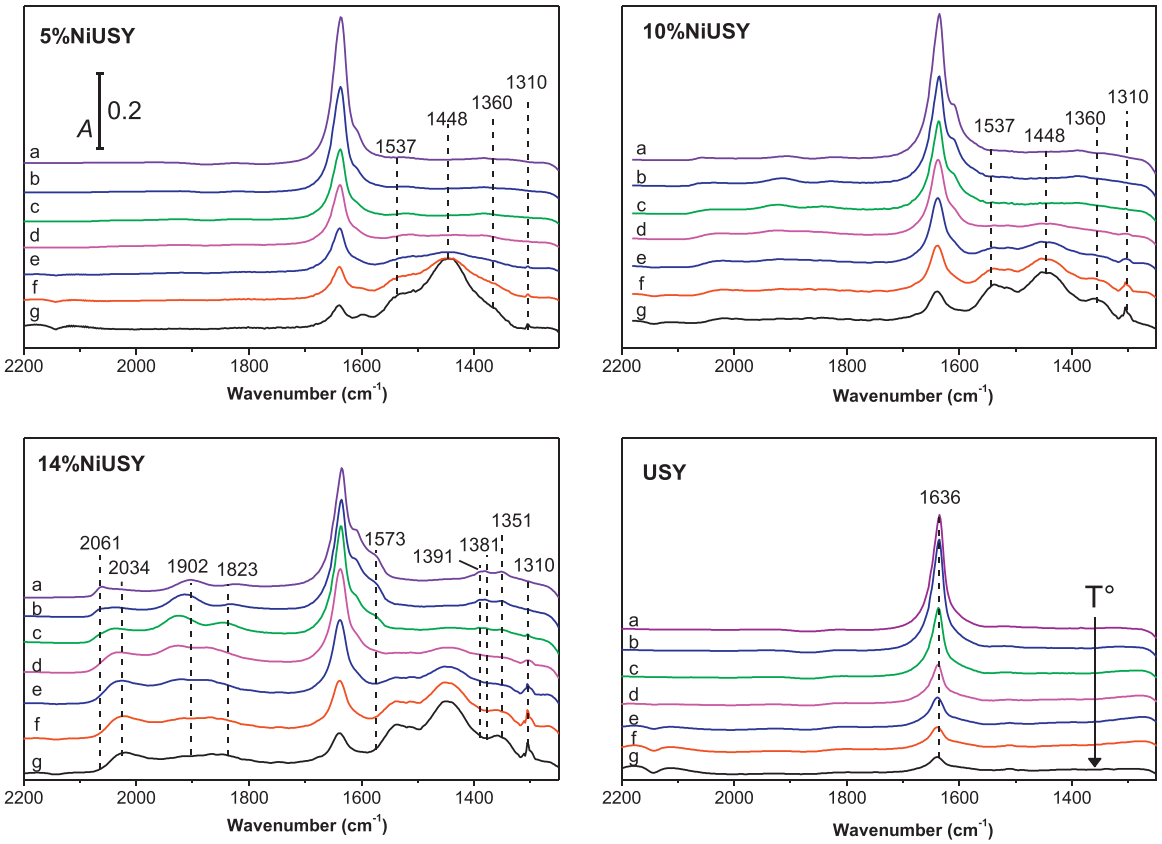

Fig. 3. - FTIR spectra under CO_2 methanation conditions over 5% NiUSY, 10% NiUSY, 14% NiUSY and USY zeolites; (a) 150 °C, (b) 200 °C, (c) 250 °C, (d) 300 °C, (e) 350 °C, (f) 400 °C, (g) 450 °C. (For interpretation of the references to color in this figure legend, the reader is referred to the web version of this article.)

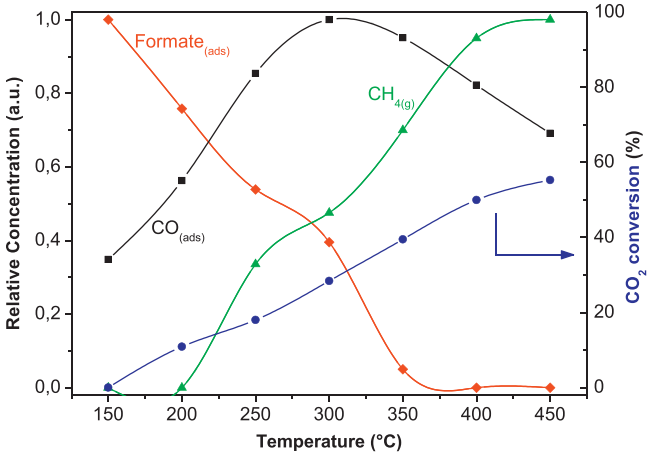

Fig. 4. - Evolution of the relative concentrations of $CH_{4(g)}$, adsorbed CO (2100–1740 cm^{-1}) and formates (1573 cm^{-1}) and CO_2 conversion (%) during TPSR Ar/H_2/CO_2 (75/20/5) over 14% NiUSY zeolite. (For interpretation of the references to color in this figure legend, the reader is referred to the web version of this article.)

FTIR (left axis) and the CO_2 conversion percentage (right axis). The semi-quantitative evolution methodology is based both on the absorbance measurement or integration of the corresponding IR band according to the presence (or not) of overlapping. Hence, the formate quantification was made by following the absorbance at $\nu = 1573\ cm^{-1}$ whereas the CO, CO_2 and CH_4 quantifications were made respectively thanks to the integrations of the respective ranges: 2100–1750 cm^{-1}, 2450–2250 cm^{-1} and 3200–2800 cm^{-1}. In all cases, the highest value measured for each species was set arbitrarily to 1 in order to obtain normalized data and allowing a better comparison between the evolutions of each component. Regarding the evolution of CO, the relative quantification takes into account all types of CO (monodentate, bidentate and bridged) since the separated quantification is not possible.

To better describe the Fig. 4, the different observations are discussed according to several temperature ranges:

- At $T \leq 200\,^{\circ}C$, it is worth noting that adsorbed formates and carbonyls adopt symmetric evolutions between 150 and 250 °C. This observation brings evidence that CO arises from formate.
- At $200 \leq T \leq 300\,^{\circ}C$, adsorbed formates and gaseous methane present close profiles with an inflexion in their evolutions. In this temperature range, the system energy starts to be high enough to dissociate then hydrogenate or to hydrogenate directly CO until the formation of methane. In addition, one can wonder if the relative high concentration of adsorbed CO limits the formate dissociation, and hence the methane formation. Indeed, as shown in other studies [16], the C—O dissociation is the rate-determining step of the methanation reaction. It could confirm the following sequence: $HCOO^-_{(ads)} \rightarrow CO_{(ads)} \rightarrow CH_{4(g)}$ and explain the relative high concentration of adsorbed CO.
- At $300 \leq T \leq 350\,^{\circ}C$, the CO concentration reaches a maximum. At this point, the relative high concentration of CO on the surface can limit its dissociation/hydrogenation (regarding a Langmuir–Hinshelwood mechanism). In addition, at 300 °C the CO concentration being maximum, the formate dissociation becomes limited. Hence, we assume that from this temperature, remaining formates can also be directly hydrogenated into CH_4 (Scheme 1), explaining the sudden drop of the concentration, while the CH_4 concentration keeps increasing.
- From $T \geq 350\,^{\circ}C$, new active sites are now available since all formates were hydrogenated into methane. Hence, CO can be dissociated/hydrogenated again and its concentration starts to decrease while the methane formation keeps increasing. Regarding the respective evolution of CO and methane with the temperature, it appears that methane formation is limited both by the rate-determining step (dissociation/hydrogenation of CO) but also by the thermodynamic (Fig. 1-B).

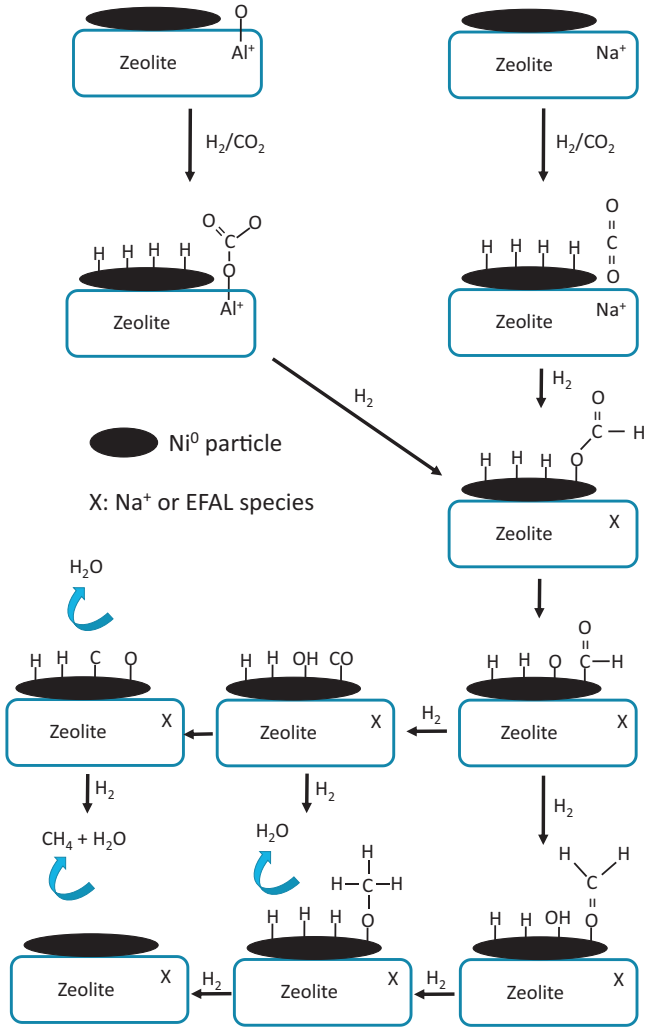

Scheme 1. - Proposed mechanism for CO_2 hydrogenation on NiUSY zeolites. (For interpretation of the references to color in this figure legend, the reader is referred to the web version of this article.)

In that way, one possible mechanism for CO_2 hydrogenation over NiUSY zeolite is shown in Scheme 1. In absence of hydrogen, CO_2 can be linearly adsorbed (*via* electrostatic interactions) onto exchangeable cations (*e.g.*, Na^+) or as monodentate carbonates onto EFAL or Ni^0 species (as revealed also by CO_2-TPD). At 150 °C, in presence of hydrogen, these species react with dissociated hydrogen to form monodentate formates adsorbed onto Ni^0. Until 300 °C, formates are almost exclusively dissociated to carbonyls, since the CH_4 formation is quite low. The increase of Ni contents implies more adsorption sites, leading to more adsorbed formates (as revealed by the increase of the band at 1573 cm^{-1}). Thus, in absence of basic sites or basic behavior of the zeolite, carbonates are probably not directly hydrogenated to methane (compared with the mechanism by Aldana et al. over Ni/Ceria–Zirconia catalysts [11] or Pan et al. [10] over Ni/Alumina) but the mechanism passes mainly through the formation of formates and then carbonyls. Nevertheless, it seems that the formation of carbonyls at high temperatures (typically above 350 °C) can also arise from the CO_2 disproportionation/dissociation onto metallic species. Carbonyl and formyl species are further hydrogenated onto Ni^0 particles to form probably formaldehyde-type and methoxy species (not observed) and in-fine methane. Finally, since we could not observe the dissociation/hydrogenation by FTIR spectroscopy, it cannot be excluded the direct CO dissociation (promoted in presence of H_2 [16]) onto Ni particles, leading to adsorbed C and O atoms, which are further hydrogenated respectively to CH_4 and H_2O.

4. Conclusions

In this study, several *operando* IR measurements were performed under CO_2/Ar or CO_2/H_2/Ar conditions onto Ni-impregnated zeolites (with increasing Ni content). It appears that, in absence of hydrogen, CO_2 is almost not adsorbed over acidic zeolite but formates and carbonyls were detected in presence of hydrogen. Hence, the CO_2 hydrogenation mechanism does not probably pass through the carbonate formation as intermediate, but rather passes through the formate dissociation onto Ni^0 particles leading at low temperatures to the formation of adsorbed CO and in a minor way to methane. Considering the absence of basic sites, CO seems to be the "true" intermediate in the CO_2 methanation reaction. The simultaneous measurements of both adsorbed and gaseous species seems to confirm previous conclusions in the literature indicating that the CO dissociation/hydrogenation is the rate-determining step for the CO_2 methanation. In addition, the methane formation seems also to be controlled by the relative concentration of adsorbed species. Hence, this mechanism can explain the much better activity by increasing the Ni content, since the increase of reduced Ni offers new adsorption sites for CO adsorption and CO/H_2 dissociation.

Acknowledgements

This work was supported by the Framework 7 program, under the project CEOPS – CO2 – loop for energy storage and conversion to organic chemistry processes through advanced catalytic systems (FP7-NMP-2012-309984).

References

[1] C. Song, Catal. Today 115 (2006) 2–32.
[2] K. Aleklett, M. Höök, K. Jakobsson, M. Lardelli, S. Snowden, B. Söderbergh, Energ. Policy 38 (2010) 1398–1414.
[3] CO_2 emissions from fuel combustion – highlights, IEA – Statistics, International Energy Agency, 2009.
[4] X.D. Xu, J.A. Moulijn, Energ. Fuel 10 (1996) 305–325.
[5] J. Ma, N. Sun, X. Zhang, N. Zhao, F. Xiao, W. Wei, Y. Sun, Catal. Today 148 (2009) 221–231.
[6] G. Centi, S. Perathoner, Catal. Today 148 (2009) 191–205.
[7] J. Kopyscinski, T.J. Schildhauer, S.M.A. Biollaz, Fuel 89 (2010) 1763–1783.
[8] C. Deleitenburg, A. Trovarelli, J. Catal. 156 (1995) 171–174.
[9] A.M. Abdel-Mageed, S. Eckle, H.G. Anfang, R.J. Behm, J. Catal. 298 (2013) 148–160.
[10] Q.S. Pan, J.X. Peng, T.J. Sun, D.N. Gao, S. Wang, S.D. Wang, Fuel Process Technol. 123 (2014) 166–171.
[11] P.A.U. Aldana, F. Ocampo, K. Kobl, B. Louis, F. Thibault-Starzyk, M. Daturi, P. Bazin, S. Thomas, A.C. Roger, Catal. Today 215 (2013) 201–207.
[12] I. Graca, L.V. Gonzalez, M.C. Bacariza, A. Fernandes, C. Henriques, J.M. Lopes, M.F. Ribeiro, Appl. Catal. B-Environ. 147 (2014) 101–110.
[13] D.J. Darensbourg, C. Ovalles, Inorg. Chem. 25 (1986) 1603–1609.
[14] S. Tada, O.J. Ochieng, R. Kikuchi, T. Haneda, H. Kameyama, Int. J. Hydrogen Energy 39 (2014) 10090–10100.
[15] A. Karelovic, P. Ruiz, Acs Catal. 3 (2013) 2799–2812.
[16] E. Jwa, S.B. Lee, H.W. Lee, Y.S. Mok, Fuel Process Technol. 108 (2013) 89–93.
[17] J. Engbaek, O. Lytken, J.H. Nielsen, L. Chorkendorff, Surf. Sci. 602 (2008) 733–743.
[18] C. deLeitenburg, A. Trovarelli, J. Kaspar, J. Catal. 166 (1997) 98–107.
[19] F. Solymosi, T. Bansagi, A. Erdohelyi, J. Catal. 72 (1981) 166–169.
[20] D.B. Cao, Y.W. Li, J.G. Wang, H.J. Jiao, Surf. Sci. 603 (2009) 2991–2998.
[21] R. Bal, B.B. Tope, T.K. Das, S.G. Hegde, S. Sivasanker, J. Catal. 204 (2001) 358–363.
[22] J.F. Li, R. Yan, B. Xiao, D.T. Liang, D.H. Lee, Energ. Fuel 22 (2008) 16–23.
[23] P. Galhotra, J.G. Navea, S.C. Larsen, V.H. Grassian, Energ. Environ. Sci. 2 (2009) 401–409.
[24] T. Montanari, G. Busca, Vib. Spectrosc. 46 (2008) 45–51.
[25] G.H. Li, C.A. Jones, V.H. Grassian, S.C. Larsen, J. Catal. 235 (2005) 431.
[26] S.C. Larsen, J. Phys. Chem. C 111 (2007) 18464–18474.
[27] S.U. Rege, R.T. Yang, Chem. Eng. Sci. 56 (2001) 3781–3796.
[28] E. Gallei, G. Stumpf, J. Colloid Interface Sci. 55 (1976) 415–420.
[29] M. Agnelli, H.M. Swaan, C. Marquez-Alvarez, G.A. Martin, C. Mirodatos, J. Catal. 175 (1998) 117–128.
[30] S. Haq, J.G. Love, H.E. Sanders, D.A. King, Surf. Sci. 325 (1995) 230–242.
[31] Q. Luo, T. Wang, M. Beller, H. Jiao, J. Mol. Catal. A: Chem. 379 (2013) 169–177.
[32] A. Yamakata, J. Kubota, J.N. Kondo, C. Hirose, K. Domen, F. Wakabayashi, J. Phys. Chem. B 101 (1997) 5177–5181.